International Research Journal of Engineering and Technology (IRJET) e-ISSN: 2395-0056
Volume: 04 Issue: 09 | Sep -2017 www.irjet.net p-ISSN: 2395-0072

Analysis of Low Voltage Ride through Capability of FSIG Based Wind Farm Using STATCOM

Roshan Kumar Gupta [1], Varun Kumar [2]

[1](P.G Scholar) EE Department KNIT Sultanpur, U.P (INDIA)-228118
[2] (Assistant Professor) EE Department KNIT Sultanpur, U.P (INDIA)-228118

Abstract - *A 12 MW fixed-speed wind farm has been modeled using MATLAB/Simulink software. The wind farm is connected to grid using FACTS that compensates the reactive power consumption of induction generators, and improves voltage stability when grid faults occur. The ability of the wind power plant to stay connected during grid disturbances is important to avoid a cascading effect due to lack of power. Making it necessary to introduce new code of practice, the grid operators require that wind turbines stay connected to the grid during voltage dips. Low Voltage Ride Through (LVRT) has emerged as a new requirement that system operators demand to wind turbines. This paper analyses the extent to which the LVRT capability of wind farms using squirrel cage generators can be enhanced by the use of a Static Synchronous Compensator (STATCOM). The ability of wind farms to stay connected to grid during LVRT is investigated based on E-ON NETZ grid code.*

Key Words: LVRT, Reactive Power, STATCOM, SCIG, Voltage Dips

1. INTRODUCTION

In this paper basically we are analyzing voltage in grid. Unbalanced grid voltage dips cause heavy generator torque oscillations that reduce the lifetime of the drive train. In this paper, investigations on an FSIG-based wind farm in combination with a Static Compensator under unbalanced grid voltage fault are carried out by means of theory, simulations, and measurements. A Static Compensator control structure with the capability to coordinate the control between the positive and the negative sequence of the grid voltage is proposed. The results conclude the effect of the voltage dip compensation by a Static Compensator on the operation of the FSIG based wind farm. With first priority, the Static Compensator ensures the maximum fault-ride-through enhancement of the wind farm by compensating the positive-sequence voltage. The remaining Static Compensator current capability of the Static compensator is controlled to compensate the negative - sequence voltage, in order to reduce the torque oscillations. Voltage instability in a power system occurs due to lack of adequate reactive power during grid fault. Injecting enough reactive power to the grid can enhance low voltage ride through (LVRT) capability of a wind farm and guarantees an uninterrupted operation of its units.

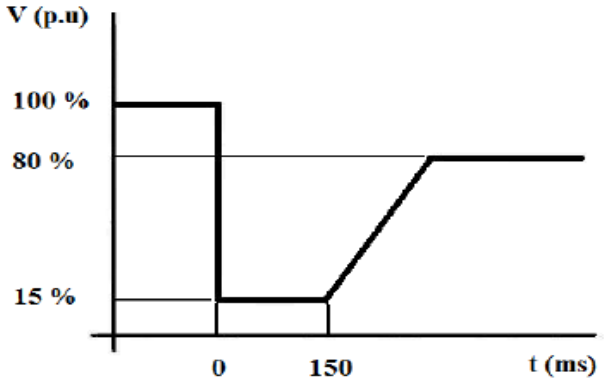

Figure 1: Voltage dips that wind turbines should be able to handle without disconnection (e.on netz).

LVRT is part of the grid code which states that wind turbines are required to remain connected to the grid for a specific amount of time otherwise they can be disconnected. This specific amount of time can be different from one grid code to another; also the severity of the fault might be different as well. Injecting reactive power for ensuring LVRT can be performed using var compensator devices such as STATCOM or capacitor banks.

The transmission utility from Germany, E.ON Netz, specifies the requirements for wind turbines connected to transmission networks of 110 kV or above. As shown in Figure1.4 the grid code regulations E.ON Netz are considered in this study. This grid code states that wind turbines must not be disconnected from the network in the event of an 85% voltage dip caused by a three-phase short circuit for 150 ms.

2. FSIG BASED WIND FARM

2.1 Description of the system

The proposed simulation model of FSIG-based WECS is shown in fig above. For this purpose the well-known platform MATLAB/SIMULINK has been used .

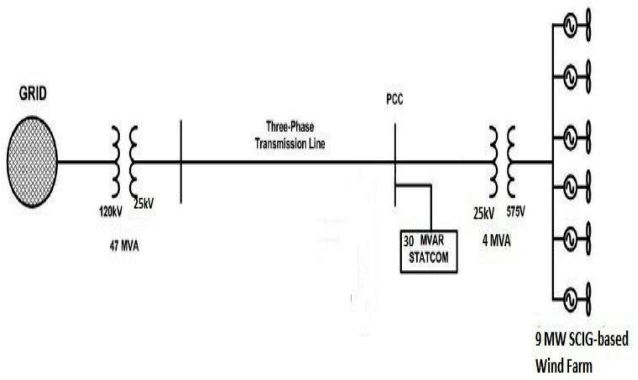

Figure 2: Block Diagram of Descripted system

A wind farm consisting of six 1.5-MW wind turbines is connected to a 25-kV distribution system exports power to a 120-kV grid through a 25-km transmission line 25-kV feeder as shown in fig above. The 9-MW wind farm is simulated by three pairs of 1.5 MW wind-turbines. Wind turbines use squirrel-cage induction generators (IG). The stator winding is connected directly to the 60 Hz grid and the rotor is driven by a variable-pitch wind turbine. The STATCOM provides reactive power support to wind generator.

2.2 Static Synchronous Compensator (STATCOM)

STATCOM is a shunt connected Fact device. Its capacitive or inductive output current is controlled independent of the ac system voltage. Fig 3: shows a simple one line diagram of STATCOM based on a voltage source converter. The voltage converter converts dc voltage to ac voltage by using power electronics devices such as GTO, MOSFET, Thyristors and the ac voltage inserted into the line using transformer. If output of the STATCOM is more than the line voltage, converter will supply lagging reactive power to the transmission line. If line voltage is more than the STATCOM output voltage then STATCOM will absorbs lagging reactive power from the system.

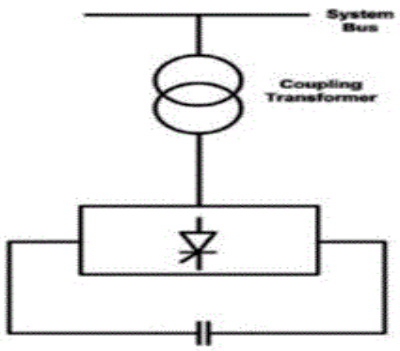

Figure 3: Static Synchronous Compensator (STATCOM)

2.3 Fixed Speed Wind Turbine

Fixed-speed wind turbines are electrically fairly simple devices consisting of an aerodynamic rotor driving a low-speed shaft, a gearbox, a high-speed shaft and an induction (sometimes known as asynchronous) generator. From the electrical system viewpoint they are perhaps best considered as large fan drives with torque applied to the low-speed shaft from the wind flow. Fig 4 illustrates the configuration of a fixed-speed wind turbine.

It consists of a squirrel-cage induction generator coupled to the power system through a turbine transformer. The generator operating slip changes slightly as the operating power level changes and the rotational speed is therefore not entirely constant. However, because the operating slip variation is generally less than 1%, this type of wind generation is normally referred to as fixed speed.

Squirrel-cage induction machines consume reactive power and so it is conventional to provide power factor correction capacitors at each wind turbine. The function of the soft-starter unit is to build up the magnetic flux slowly and so minimize transient currents during energization of the generator. Also, by applying the network voltage slowly to the generator, once energized, it brings the drive train slowly to its operating rotational speed.

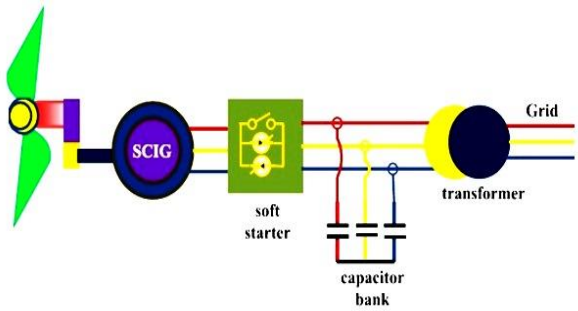

Fig 4 Schematic diagram of a fixed speed wind turbine

3. RESULTS AND DISCUSSION

CASE STUDY 3.1.1 WITH LLG (Two phase to Ground fault) FAULT AT WTG AND WITHOUT STATCOM

In this case study the parameters of three phase fault block near WTG (Wind Turbine Generator) 2 is adjusted to LLG fault condition and the STATCOM is positioned to 'Trip'. The fault is created to occur at 5 seconds. The objective of this case is to study overall dynamic and transient behaviour of the system during and after the fault at WTG.

Simulation results from bus scopes are as shown in Figure 3.1. The voltage at bus is 0.98 pu before LLG fault and after the fault it is 1.06 pu. The real power reached its steady

value of 9 MW after 4.9 seconds and immediately after the fault, real power drops to zero at 5.1 seconds. The reactive power at PCC is 3 MVAr before fault and after the occurrence of fault it is -0.25 MVAr.

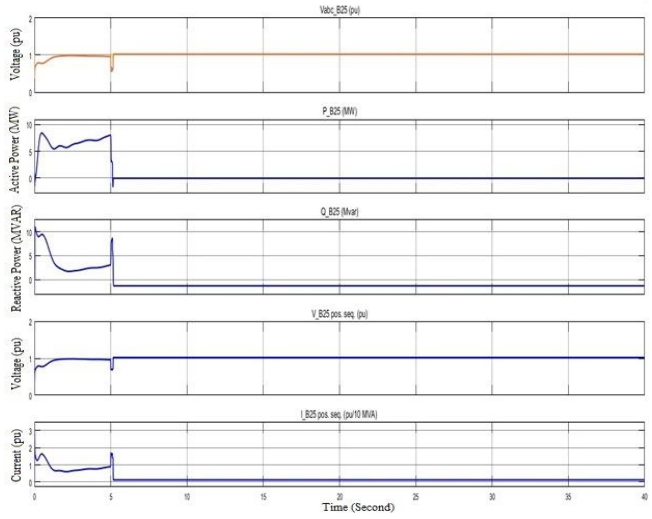

Fig 3.1. Waveform of Voltage (pu), Active power (MW), reactive power (Mvar), Positive sequence voltage (pu) and Positive sequence current (pu) at PCC for the case with fault at WTG and without STATCOM

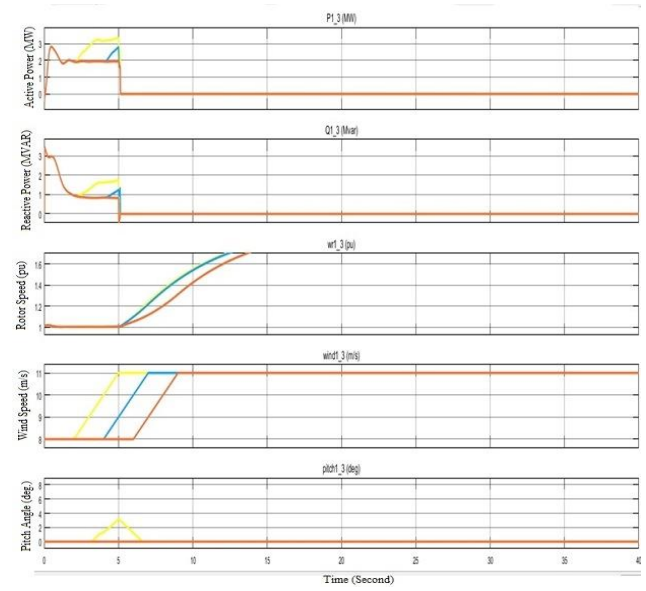

Fig 3.2. Waveform of Active power (MW), reactive power (Mvar), rotor speed (pu), wind speed (m/s) and Pitch angle (deg.) at wind turbine 1, 2, 3 respectively for the case with fault at WTG and without STATCOM

The scopes obtained after simulation on the details of wind turbine is shown in Figure 3.2. The real power developed is 3 MW by each WTG and a total of 9 MW and reactive power of 1.5 MVAr by each turbine until 5 second. After the occurrence of the fault, both real power and reactive power reaches zero. The pitch angle drops to zero at 7 seconds after the fault occurrence.

CASE STUDY 3.1.2 WITH LLG FAULT AT WTG AND WITH 3 MVAR– STATCOM

In this case STATCOM is used to get reactive power support at PCC. The fault has been created to occur at 5.15 seconds and the objective of this case is now to check the behavior of the system during LLG fault at WTG and to find inclusion of STATCOM brings any change in such cases. Simulation results from bus scopes are as shown in Figure 3.3. The voltage at PCC has improved to 0.985pu before LLG fault and

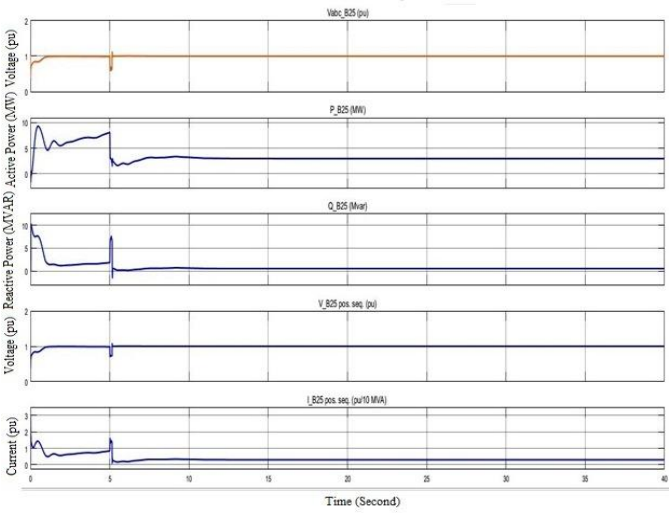

Fig 3.3. Waveform of Voltage (pu), Active power (MW), reactive power (Mvar), Positive sequence voltage (pu) and Positive sequence current (pu) at PCC for the case with fault at WTG, with 3 MVAR –STATCOM

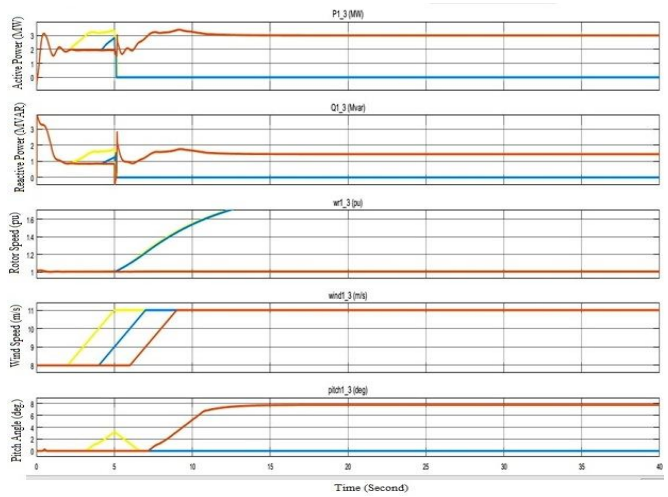

Fig 3.4. Waveform of Active power (MW), reactive power (Mvar), rotor speed (pu), wind speed (m/s) and Pitch angle (deg.) at wind turbine 1, 2, 3 respectively for the case with fault at WTG and with 3MVAR STATCOM

after the fault it is 1.06 pu. The real power reached its value of 8 MW after 5 second and after 5.15 seconds the real power goes down to zero. The reactive power is 2 MVAr before fault and it is 0.8 MVAr after the occurrence of fault. Even with the support of 3 MVAr STATCOM, at PCC reactive power absorption is observed.

The scopes obtained after simulation on the details of wind turbine is shown in Figure 3.4. The real power developed is 3 MW by each WTG and a total of 9 MW and reactive power of 1.5 MVAr by each turbine until 5 seconds. After the occurrence of the fault, both real power 6 MW and 3MVAr reactive power.

CASE STUDY 3.1.3.WITH LLG FAULT AT WTG AND WITH 30MVAR–STATCOM

In this case the rating of the STATCOM is increased from 3 MVAr to 30 MVAr. The fault is created to occur at 5 seconds. Simulation results from bus scopes are as shown in Figure 3.5

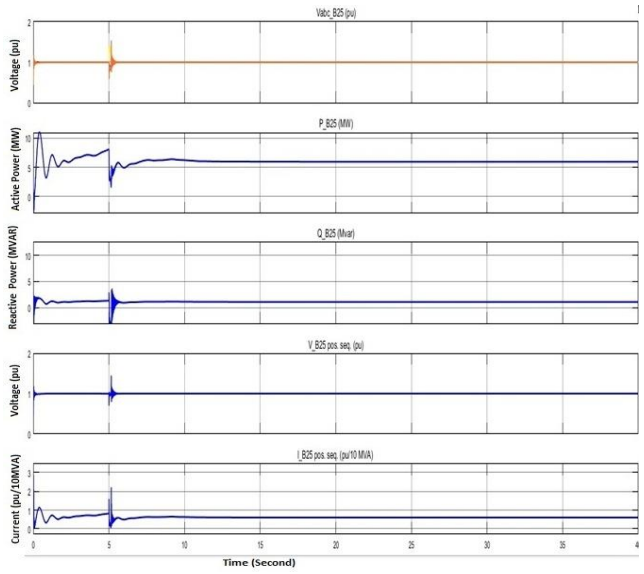

Fig 3.5. Waveform of Voltage (pu), Active power (MW), reactive power (Mvar), Positive sequence voltage (pu) and Positive sequence current (pu) at PCC for the case with LLG fault at WTG, with 30 MVAR –STATCOM

The voltage at bus is 0.998 pu before LLG fault and after the fault it is 1.01 pu. The real power reaches value of 8 MW befor 5 sec and as the fault occurs at 5.15 seconds the real power goes down to zero during fault. The reactive power is 2 MVAr before fault and after the occurrence of fault it is 2 MVAr. 30 MVAr STATCOM support the system with LLG fault.

The scopes obtained after simulation on the details of wind turbine are shown in Figure 3.4 and 3.5 respectively and not much change from the previous case is observed. The generated reactive power is about 1.5 MVAr by each turbine before fault and after fault it is 1.5 MVAr by Two turbines. It indicates that absorption of reactive power is less than generation by the system with the support of STATCOM, so the system is able to ride through the LLG fault.

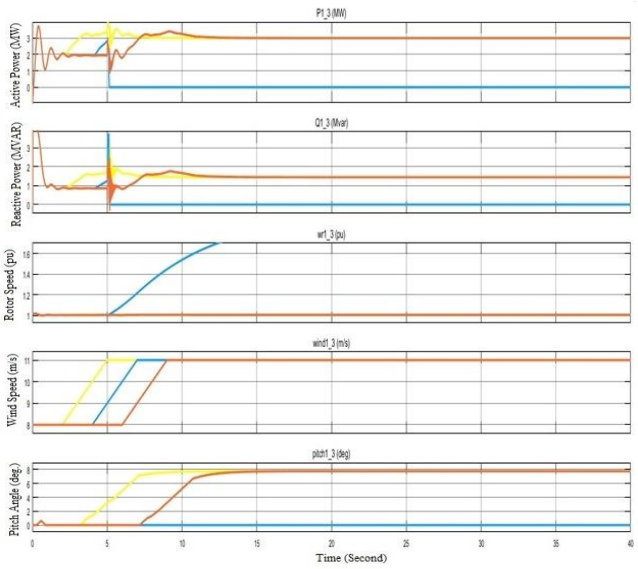

Fig 3.6 Waveform of Active power (MW), reactive power (Mvar), rotor speed (pu), wind speed (m/s) and Pitch angle (deg.) at wind turbine 1, 2, 3 respectively for the case with fault at WTG and with 30MVAR STATCOM

3.2 Comparative performance study of test system with and without STATCOM during fault duration

CASE STUDY 3.2.1: Without fault at WTG

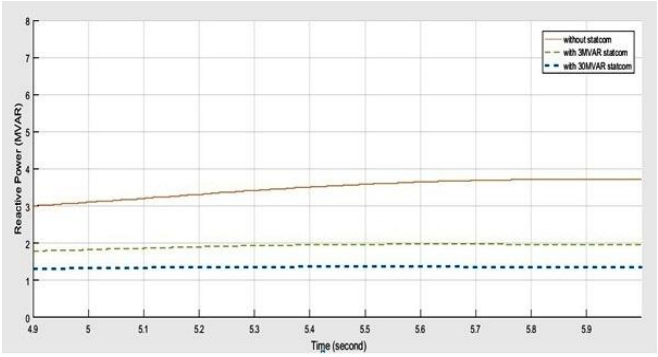

Fig. 3.7 The Reactive Power at BUS B25 with and without STATCOM.

To study the effect of STATCOM on the steady state operation, the operation of the wind farm is monitored twice, one without STATCOM and the other with STATCOM connection at the main bus B25 of the wind farm. Figure 3.7 shows that, the absorbed reactive power from the grid is 1.98 MVAR when the STATCOM is disconnected. The absorbed reactive power is decreased to 1.28 MVAR in case

of 3 MVAR STATCOM and it decreases to 1.39 MVAR in case of 30 MVAR STATOM.

Figure 3.8 shows that the voltage of the main bus of the wind farm B25 increased from 0.945 to 0.985 pu with 3 MVAR STATCOM connection and it increases to 0.998 pu with 30 MVAR STATCOM connection. Figure 3.7 shows that the total generated active power from the wind farm is increased

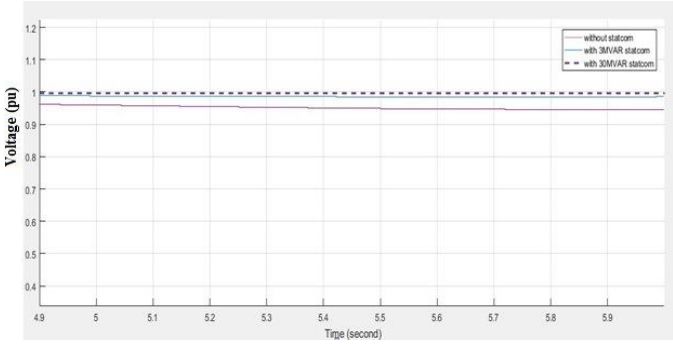

Fig. 3.8 The voltage at BUS B25 with and without STATCOM.

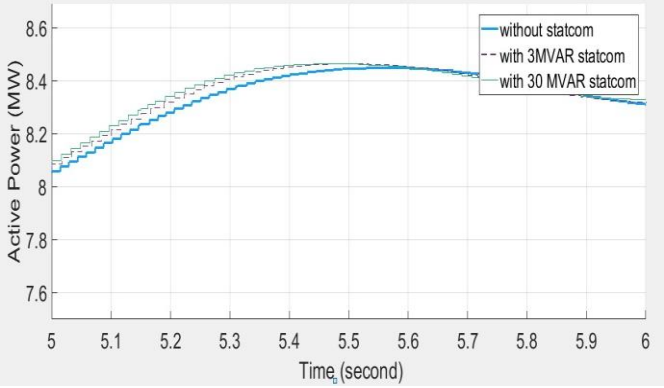

Fig. 3.9 The Active Power at BUS B25 with and without STATCOM.

From 8.15 MW to 8.16 MW with 3 MVAR STATCOM while it is increased to 8.17 MW in the case of 30 MVAR STATCOM. It is clear that, STATCOM makes to decrease the absorbed reactive power from the grid, raising the voltage of the main bus of the wind farm and also increasing the total generated active power from the wind farm.

CASE STUDY 3.2.2: With LLG at WTG

Figure 3.10 shows that the total generated active power from the wind farm during voltage dip period is decreased in case of with 30 MVAR STATCOM connection then returns back to its rated value after the end of the post disturbance period, while in case of without STATCOM connection the total generated active power during voltage dip period is decreased and falls to zero where the protection system trips the wind farm.

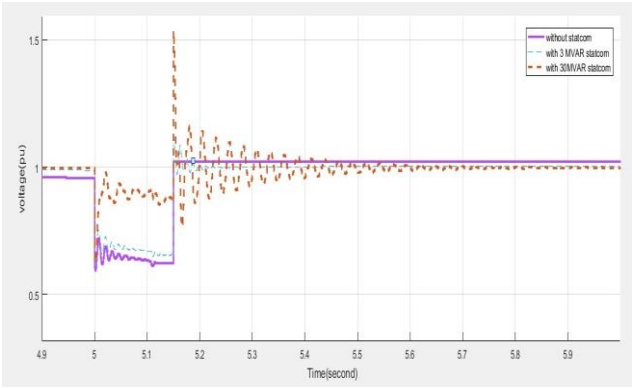

Fig. 3.10 The voltage at BUS B25 with and without STATCOM.

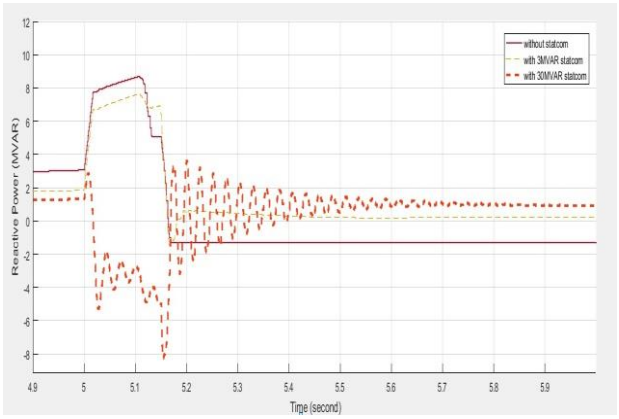

Fig. 3.11 The Reactive Power at BUS B25 with and without STATCOM.

Figure's 3.9, 3.10 and 3.11 show that, in case of without STATCOM or 3 MVAR STATCOM connection, the protection system trips the wind farm because the under voltage duration time exceeding the protection delay time. But in case of with 30 MVAR STATCOM connection, the wind farm stays in service and the system returns back to steady state after the end of the post disturbance period.

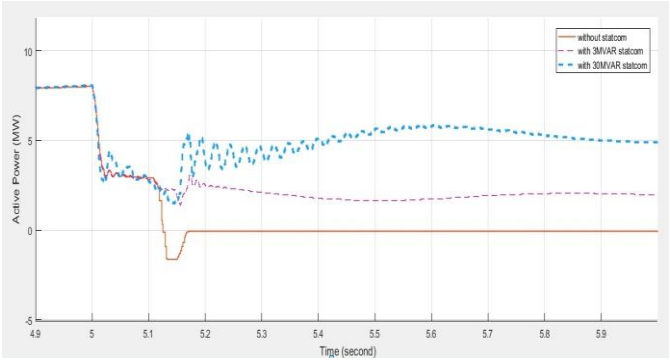

Fig. 3.12 The Active Power at BUS B25 with and without STATCOM

Table 3.4 Comparative analysis of FSIG based wind farm during fault duration

Without fault and with/without STATCOM (MVAR)				With fault LLG and with / without STATCOM		
0		**3**	**30**	**0**	**3**	**30**
Reactive Power (MVAR)	3.2	1.8	1.2	7.78	6.25	-5.6
Active Power (MW)	8.15	8.17	8.18	0.0	3.12	5.98
Voltage (pu)	0.96	0.97	1.01	0.6	0.7	0.98

4. Conclusion

To study the effect of the disturbance state, the operation of the wind farm under voltage dip in the grid side is monitored twice, one when the voltage dip occurs without STATCOM connection and the other when the voltage dip occurs with 3 MVAR and 30 MVAR STATCOM connection. In this paper the simulated disturbance starts at the fifth second, for 150 ms duration according to the studied required grid code E.ON Netz.

Without Fault at WTG and Without STATCOM The real power developed by each WTG is 3 MW adding to the total capacity of 9 MW. It also shows that the system reaches its steady state after 8 seconds but with 3MVAR STATCOM the reactive power at PCC dropped from 4 MVAr to 2.5 MVAr due to reactive compensation and The system reached its steady state after 7 sec. STATCOM rating is adjusted to 30 MVAr and this rating was taken to observe possibility of any major improvement.

With LLG Fault at WTG and Without STATCOM the capacity of the STATCOM is not enough for SCIG based wind farm to ride-through the fault and the maximum PCC voltage is around 0.64 p.u. and after the fault is cleared STATCOM capacity is enough to keep the voltage between ±5% of nominal voltage in normal operation of the power system. With 3MVAR STATCOM The capacity of the STATCOM is little enough for SCIG based wind farm to ride-through the fault and the maximum PCC voltage is around 0.7 p.u. after the fault is cleared some of the generator start delivering power. With 30MVAR STATCOM The voltage at bus is 0.992 pu before LLG fault and after the fault it is 1.01 pu. The real power reaches value of 8 MW after 5 sec and as the fault occurs at 5.15 seconds the real power goes down to zero during fault. The reactive power is 2 MVAr before fault and after the occurrence of fault it is -4.5 MVAr. 30 MVAr STATCOM support the system with LLG fault.

The major contributions of this paper is :

1) The result shows that the wind farm needs a STATCOM to provide reactive power in weak grid.

2) A practical method to obtain the minimum rating of STATCOM for fast voltage recovery at the PCC after the fault is removed was proposed and tested for different grid conditions.

5. APPENDIX

Table 5.1 Parameters of FSIG-based WECS

Parameter	Value
Nominal active power	1.5 MW
Grid voltage	120 kV
Grid frequency	60 Hz
Distribution line voltage	25 kV
Wind turbine bus voltage	575 V
Stator resistance Rs	0.0048 p.u.
Stator leakage inductance Ls	0.1248 p.u.
Rotor resistance Rr	0.0044 p.u.
Rotor leakage inductance Lr	0.1791 p.u.
Mutual Inductance Lm	6.77 p.u.
System inertia constant H	5.04
Generator friction factor F	0.01 p.u.
Generator pairs of poles P	3

Table 5.2 Transmission line parameters:

Parameter	Positive Sequence	Zero Sequence
Resistance	0.04 Ω/Km	0.12 Ω/Km
Inductance	1.05 mH/Km	3.32 mH/Km
Capacitance	11.33 nF/Km	5.01 nF/Km

Table 5.3 Control parameters

Parameter	Value
Transmission distance	25 km
Turbine pitch controller gains	Kp = 5, Ki = 25
FSIG capacitive reactive power compensator	400 KVar
STATCOM DC link nominal voltage	Kv = 4
3 MVA STATCOM DC link total capacitance	375 × 3 μ F
3MVA STATCOM AC voltage regulator gains	Kp = 5, Ki = 1000
STATCOM DC voltage regulator gains	Kp = 0.0001,Ki = 0.02
STATCOM current regulator gains	Kp =0.3, Ki =10, K_f =0.22

REFERENCES

[1] P.J. Musgrove, "Wind energy conversion an introduction", IEE Proceedings on Physical Science, Measurement and Instrumentation, Management and Education, Reviews, vol. 130, no.9, pp. 506-516, 1983.

[2] B. K. Bose, "Power Electronics and Motor Drives Recent Progress and Perspective". IEEE Transactions on Industrial Electronics, vol. 56, no. 2 pp. 581- 588, 2009.

[3] C. G. Anderson, J. B. Richon, T. J. Campbell, "An Aerodynamic Moment- Controlled Surface for Gust Load Alleviation on Wind Turbine Rotors", IEEE Transactions on control systems technology, vol. 6, no.5, pp.577-595, 1998.

[4] E. Muljadi, C.P. Butterfield, "Pitch-controlled Variable-speed Wind Turbine Generation", IEEE Transactions on Industry Applications, vol. 37, no.1, pp. 240- 246 , 2001.

[5] T. Thiringer, J. Linders, "Control by Variable Rotor Speed of a Fixed-Pitch Wind Turbine Operating in a Wide Speed Range", IEEE Transactions on Energy Conversion, vol. 8, no. 3, pp. 520-526, 1993.

[6] Y. Xingjia, L. Yingming, X. Zuoxia, Z. Chunming, "Active Vibration Control Strategy Based on Expert PID Pitch Control of Variable Speed Wind Turbine", IEEE International Conference on Electrical Machines and Systems, pp. 635-639, 17-20 Oct. 2008.

[7] R. Datta, V.T. Ranganathan, "Variable Speed Wind Power Generation Using Doubly Fed Wound Rotor Induction Machine-A Comparison with Alternative Schemes", IEEE Transaction on Energy Conversion, vol. 17, no.3, pp. 414-421, 2002.

[8] R. Takahashi, J. Tamura, "Frequency Control of Isolated Power System with Wind Farm by Using Flywheel Energy Storage System", IEEE Proceedings on Electrical Machines, pp.1-6, 6-9 Sep. 2008.

[9] D.S. Brereton, D.G. Lewis, C. G. Young, "Representation of Induction Motor Loads during Power System stability studies", AIEE Transactions on Power Apparatus and Systems, vol. 76, no.3, pp. 451-461, 1957.

[10] H. C. Stanley, "An Analysis of the Induction Motor", AIEE Transactions, vol. 57, no.12, pp.751-755, 1938.

[11] T.J. Hammons, "Voltage Dips Due to Direct Connection of Induction Generators in Low Head Hydro Electric schemes", IEEE Transactions on Energy Conversion, vol. 9, no.3, pp. 460-465, 1994.

[12] C. S. Demoulias, P. S. Dokopoulos, "Electrical Transients of wind Turbines In a Small Power Grid", IEEE Transactions on Energy Conversion, vol. 11, no. 3, pp. 636-642, 1996.

[13] C. S. Demoulias, P. S. Dokopoulos, "Transient Behavior and Self-Excitation of Wind-Driven Induction Generator after its Disconnection from the Power Grid", IEEE Transactions on Energy Conversion, vol. 5, no. 2, pp. 272-278, 1999.

[14] L. Tang, R. Zavadil, "Shunt Capacitor Failures Due to Wind Farm Induction Generator Self-excitation Phenomenon", IEEE Transactions on Energy Conversion, vol. 8, no. 3, pp. 513-519, 1993.

[15] T. Petru, T. Thiringer, "Modeling of Wind Turbines for Power System Studies", IEEE Transactions on Energy Conversion, vol. 17, no. 4, pp. 1132-1139, 2002.

[16] L. M. Popa, F. Blaabjerg and I. Boldea, "Wind Turbine Generator Modeling and Simulation Where Rotational Speed is the Controlled Variable", IEEE Transactions on Industry Applications, vol. 40, no.1 pp. 3-10, 2004.

[17] B. H. Khan, "Non-Conventional Energy Resources" Mc Graw Hill publication 2012.

[18] C. Jauch, J. Matevosyan, T. Ackermann, and S. Bolik, "International comparison of requirements for connection of wind turbines to power systems", Wind Energy, vol. 8, pp. 295–306, 2005.

[19] Seman, S., Niiranen, J., Arkkio A., "Ride-Through Analysis of Doubly Fed Induction Wind-Power Generator Under Unsymmetrical Network Disturbance", Power Systems, IEEE Transactions on Volume 21, Issue 4, Nov. 2006 Page(s):1782 – 1789.

[20] World Wind Energy Association "Uniting the world of wind energy since 2001" publication August 2011.

[21] Dr. S. Gomathinayagam "Introduction to the Indian Wind Energy Sector" Shri Venugopal Pillai, "Revolution in the Air", Electrical Monitor, Oct. 2009, PP. 30-37.

[22] M. Tsilli, Ch. Patsiouras, S. Papathanassiou, "Grid Code Requirement for large wind farms: A review of technical regulations and available wind turbine technologies", National Technical University of Athens (NTUA) School of Electrical and Computer Engineering.

[23] Centre for Wind Energy Technology Chennai "Indian Wind Grid Code".

[24] Matlab R2012a, "Wind Turbine demonstrations".